AO-4025 ITT ESA – Surface Treatment and Coating for the Reduction of Multipactor and Passive Intermodulation (PIM) Effects in RF Components

D. Wolk[1], J. Damaschke[1], C. Vicente[2], B. Mottet[2], H.L. Hartnagel[2], L. Galán[3], I. Montero[4], E. Roman[4], M. Alfonseca[5], J. de Lara[5], D. Raboso[6],

[1)] *Tesat Spacecom GmbH & Co. KG*
Gerberstr. 49, D-71522 Backnang, Germany

[2)] *Institut für Hochfrequenztechnik, TU Darmstadt*
Merckstr. 25, D-64283 Darmstadt, Germany

[3)] *Departamento de Fisica Aplicada, Universidad Autónoma de Madrid*
28049-Madrid, Spain

[4)] *Instituto de Ciencia de Materiales de Madrid, CSIC*
28049-Madrid, Spain

[5)] *Escuela Tecnica Superior de Informatica, Universidad Autónoma de Madrid*
28049-Madrid, Spain

[6)] *ESA/ ESTEC*
Keplerlaan 1, 2200 AG Noordwijk, The Netherlands

Abstract

ESA has initiated several activities with the aim to reduce the risk of multipaction and corona effects in space hardware. Within the activity "Surface Treatment and Coating for the Reduction of Multipactor and Passive Intermodulation (PIM) Effects in RF Components" a European group has been formed to investigate new surface coatings / treatments to improve the power handling capability of passive equipment with respect to multipactor and passive intermodulation. This paper presents an overview of the activities to be performed within this project and describes the first results.

1 Introduction

New satellite payloads are operated with an extremely high number of communication channels and a still increasing power level per channel. Therefore the risk of multipactor discharge and increased passive intermodulation level for the payload performance and reliability is increasing. The purpose of this study is to select coating materials, deposition techniques and surface treatments for the reduction of multipactor. Potential selected coatings will be investigated with respect to RF-performance. A secondary emission software will be created which allows to predict the effect of secondary emission and conductivity of surface coatings on multipactor and RF-performance. Technology and RF waveguide samples will be characterized, measured and the results will be compared with the predictions.
A similar route will be followed for the PIM effect. Coating materials and surface machining techniques for the minimisation of passive intermodulation level will be studied. Several analysis techniques will be applied to characterise the surfaces. A software will be created which allows to predict the intermodulation level for a given excited frequency as a function of system parameters like signal power in dependence of the physical properties of the coating material. Samples in waveguide techniques will be manufactured and measured. Results will be compared with the predictions.
For the multipaction testing, especially in the pulsed / multicarrier case, an electron source is required to provide a sufficient amount of seeding electrons. One of the objectives of this contract is the development of a computer controlled regulated source. An electron gun is foreseen for this purpose. The energy, the current and the density of the electron beam can be regulated.
This activity is closely related to another ESA activity. Within the contract "Multipactor and Corona Discharge: Simulation and Design in Microwave Components" [16] a software tool will be developed which allows to predict more accurately the onset of multipaction and corona effects in waveguide structures and to verify these results by experimental hardware.
This paper is organised in function of the activities performed by each of the partners.
Tesat-Spacecom is in charge for design and manufacturing of the REG and of the multipaction samples. Verification Tests (multipaction and PIM) will be performed at Tesat-Spacecom facility. UAM Madrid is the partner for the study of the secondary emission properties of surfaces and for the coating. TUD is in charge for the development of a PIM software and the PIM samples design.

2 Secondary Electron Emission and Multipactor Effect; Contribution of UAM Madrid

2.1 General

The search for reliable low-secondary-electron-emission coatings is considered as one of the main research lines to reduce the multipactor effect in high-power RF devices in spacecraft and in other important technological fields as high energy particle accelerators. Previous ESTEC studies[1-5] revealed that to correlate secondary emission (SEY) and multipactor threshold (MPT) is complicated because both measurements cannot be made in situ and simultaneously. Mainly for coatings of low SEY, this property is highly sensitive to air exposure, electron or ion bombardment, ... etc, so the SEY properties measured in the surface laboratory might change when tested for MPT. Because of this and for applications, it is of great interest to simulate adequately the SEY process in a computer model of the multipactor effect.

Both experimental[6] and preliminary computer simulation results[7] indicate that the electron energies in the multipactor discharge are mostly below the RF peak gap voltage. Thus, for SEY, the range of interest of primary electron energies is below 2000 eV. They show also that the main parameters of SEY influencing multipactor are the maximum value σ_m of SEY coefficient and the first crossover primary energy E_1 ($\sigma(E_1) = 1$). Their values measured at normal incidence can be correlated with MPT, Fig. 1

When surface conditioning for multipactor or testing for multipactor threshold RF equipment, this threshold is reached and the discharge is allowed to occur. During this process the surfaces exposed to the discharge are bombarded with electrons and ions (depending on the vacuum) accelerated by the RF field. Thus, the behaviour of SEY under electron bombardment (electron conditioning) is of great interest. Probably, when testing for MPT, some partial electron conditioning always occurs. The strong influence of electron conditioning on SEY (see Table I) was probably the main reason for a relatively poor correlation between SEY properties and MPT test results[1-5]. This correlation is improved using mean values between air-exposed and electron-conditioned ones. It is also improved if $E1$ and σ_m are combined in a figure of merit: $\sqrt{E_1/\sigma_m}$. In Fig. 1, SEY and MPT results (5.3 GHz × 2 mm) for several surfaces are shown. Extremely high values (shadowed dots) were achieved by in situ ion conditioning (RF Ar plasma) previous to MPT tests[5].

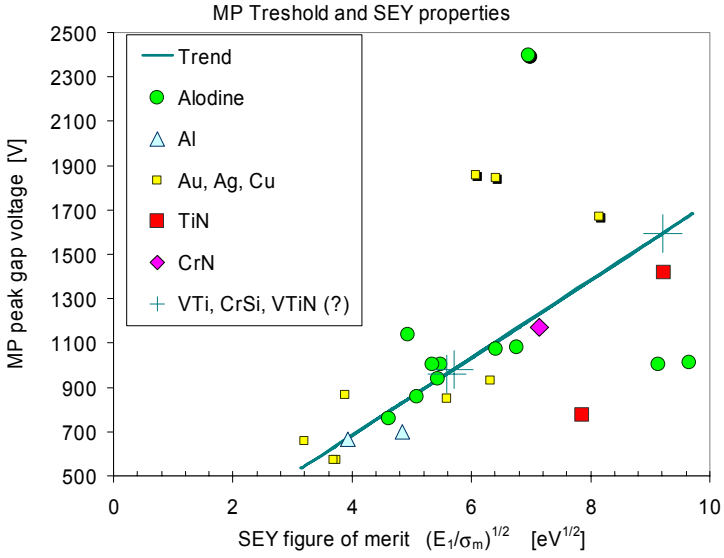

Fig. 1: Correlation between Multipactor and Secondary Emission Properties.

SEY values are an average between *air-exposed* and *electron conditioned* (*ion-conditioned* for samples ion bombarded *in situ* in ESTEC, shadowed dots). The (not measured) MP thresholds for CrSi, VTi, and VTiN are estimates from the correlation. MPT results for 5.3 GHz × 2 mm. Most data from Ref. 1 – 5.

In this article, we present some recent results of two kinds of SEY measurements. The first one is the SEY coefficient or number of secondaries produced as a function of the energy of the primary or impacting electron at normal incidence for coating materials with low SEY for applications in reducing multipactor effect. This property is the main one to be considered in an evaluation criterion for that application. It is also the main SEY property to be simulated in a computer model of the multipactor effect. As mentioned above, for more meaningful values, both air-exposed (month scale) and electron-conditioned states should be considered.

The other kind of measurements are the energy distribution curves (EDC) or energy spectra of emitted secondary electrons. Their dependence on material and on primary energy is not well known, yet thought to be small and

thus of little effect on multipactor. However, this should be proved by the computer simulation. In any case, secondary electrons in the model should have an energy and its values should be realistic. A simple simulation of this SEY property will be proposed.

2.2 Experimental

SEY measurements were performed in the analyser chamber of a surface science UHV system also having facilities for XPS and AES (surface chemical analysis and electronic structure) and a noble ion sputtering gun (depth profiling)[LH10]. Samples could be either introduced from outside, the laboratory, or deposited/treated in the preparation chamber directly attached to the analysis one.

For preparation of Cr silicides, very thin films of the metal were deposited by thermal evaporation (sublimation) on clean single-crystal Si substrates, the reaction was produced by either *ion mixing* (low energy Ar^+ ion bombarding, 2 keV) or thermal annealing. These were above 300ºC, or better by heat flashes (< 1 min) at ~ 700ºC. While Cr evaporation, partial oxidation is inevitable, however, Ar ion bombardment induces reduction of oxides by preferential sputtering of oxygen besides diffusion and reaction (*ion mixing*) at low temperature.

V 5 % Ti alloy was made by melting in a vacuum furnace. Then, samples with finely polished surfaces were prepared by the usual metallurgical techniques. After characterisation, very thin V (5%Ti) nitride coatings were grown by low-energy N_2^+ ion implantation (0.1 – 5 keV).

SEY was determined by measuring the net current to the sample when bombarded by a calibrated electron beam of adjustable energy (2 mm^2, 0.5×10^{-8} A, ΔE_p = 0.5 eV). The sample was maintained at a fix low negative potential (in a nearly field-free volume) while the electron energy was scanned. A small solid angle, 10º×10º, of the emission can be analysed in energy (SEY EDC or energy spectrum, see section below). The small negative potential on the sample was sufficient to allow using the energy range where analyser transmission function is simpler and more accurately calibrated.

2.3 Results and Discussion

2.3.1 Secondary Emission of Transition Metal Nitrides and Silicides

As important as the coating having low SEY after deposition is that the surface is passivated, reluctant to deteriorate under exposure to air. Unfortunately, this is practically impossible to attain: the surfaces with lower SEY are more reactive and increase higher its value upon exposure to oxygen and oxygen containing molecules of atmospheric air. The best thing is partial passivation of the surface by the formation of nitrides, carbides, and silicides or even suboxides.

The nitrides and carbides of light transition metals like Ti and V and pure Cr are known since several decades as materials for coatings in applications with increased multipactor breakdown levels[9]. Nitrides, carbides and silicides of transition metals are also used in microelectronics as chemical-stable low-resistivity coatings. Pure clean Ti, V, and Cr have very low SEY coefficient: $\sigma_m \approx 1.0$ or lower. Pure clean nitrides, carbides and silicides with important metallic character have similar SEY properties[10]. However, these properties degrade strongly upon exposure to air: $\sigma_m \sim 2.5$, $E_1 \sim 25$ eV, faster for the pure metals than for the compounds. High valence oxides and adsorbed water seem to be the cause. However, metal suboxides, oxinitrides, and oxicarbides with some metallic character have relatively good properties: $\sigma_m \sim 1.2$, $E_1 \sim 100 - 150$ *eV*, and probably hinder further oxidation. Oxidation rate decreases in the series Ti, V, and Cr compounds. However, also the electrical conductivity does. Partial oxidation necessary to passivate the surface will also produce an increase of the surface resistance.

In Table I, we present SEY data for some coatings comparing favourably with *Alodine 1200*, Cu is also shown as a reference. Only TiN is commonly used in coatings for reduced MPT. TiN and VN have thoroughly been studied for this application[9, 10]. CrN and light transition metal silicides were studied and proposed for this application by our laboratory[3, 4].

The VN samples studied were obtained by low-energy nitrogen ion implantation on a V 5% Ti alloy of interest in other applied fields for its tribological properties. The good SEY properties of the alloy and its nitrides even after very long air exposure are remarkable. This is a new form of a material not very frequent in multipactor applications.

SEY properties of transition metal silicides had not been studied before. We present measurements for Cr silicides in Fig. 2. These indicate that these materials have potential in low-MPT applications. Very thin coatings were deposited on clean Si substrates. The stoichiometry of these thin films was not well determined, but $CrSi_2$ was the phase expected for the deposition conditions[11]. This compound was thought to be a semiconductor, but it is rather a metal with low conductivity[11]. XPS analysis of the Cr-Si reaction supports a metallic character of the films. Experiments showed that some samples withstand long air exposures. Vanadium silicides are expected to have these good properties with better conductivity.

		σ_m	E_1 [eV]	$(E_1/\sigma_m)^{1/2}$ [$eV^{1/2}$]	V_M [V]
CrSi	Cr evaporation on Si in UHV				
	Ar^+ sputtering, bake 400ºC				
	air exposure	1.8	50	5.3	
	electron conditioning	1.3	50	6.2	
V-*Ti*	5%Ti alloy, polished				
	air exposure	1.8	40	4.7	
	electron conditioning	1.2	50	6.5	
VTiN	low energy ion implantation				
	6d air exposure	1.7	90	7.2	
	electron conditioning	1.25	155	11.1	
CrN[3, 4]	air exposure	1.7	65	6.2	1170
	electron conditioning	1.3	85	8.1	
TiN[3, 4]	7 day air exposure	1.2	150	11.1	
	air exposure	1.4	105	8.7	1420
	electron conditioning	1.15	110	9.8	
Cu[1, 2]	air exposed	2.0	30	3.9	950
	electron conditioning	1.3	80	7.8	
	ion conditioning	1.4	170	11.	1480
	electron conditioning	1.2	185	12.4	
Alodine[1, 2]	air exposed	1.7	44	4.4	970
	electron conditioning	1.3	51	6.4	
	ion conditioning	1.3	100	8.	>2100

Electron conditioning: 10^{18} cm^{-2} 500 eV electrons. Ion conditioning: 10^{17} cm^{-2} 3 keV Ar^+ ions.

Table I: SEY and MPT of some light transition metal nitrides and silicides.

All the coatings had relatively high O and C contamination either from preparation conditions or air exposure. The formation of suboxides, oxinitrides, or oxicarbides could concede them some surface passivation without impairing their SEY properties.

The highest measured multipactor threshold corresponds to TiN deposited by reactive electron-beam thermal evaporation in N_2 residual atmosphere with low energy Ar^+ ion beam assistance[3, 4]. This ion assistance was probably important in the coating properties producing a flat smooth and compact coating with a surface roughness in the nm scale. Simple or reactive evaporation ion assisted is probably a good deposition technique in all cases. Sputtering or reactive sputtering possibly ion assisted will presumably also be a good deposition technique.

Surface conditioning by low-energy electron or ion beams is not practical surface treatment after deposition processes since their effect are recovered by air exposure. They are rather techniques to study the secondary emission properties of the coating. They are very good surface treatments if applied *in situ* in the waveguide under the RF field.

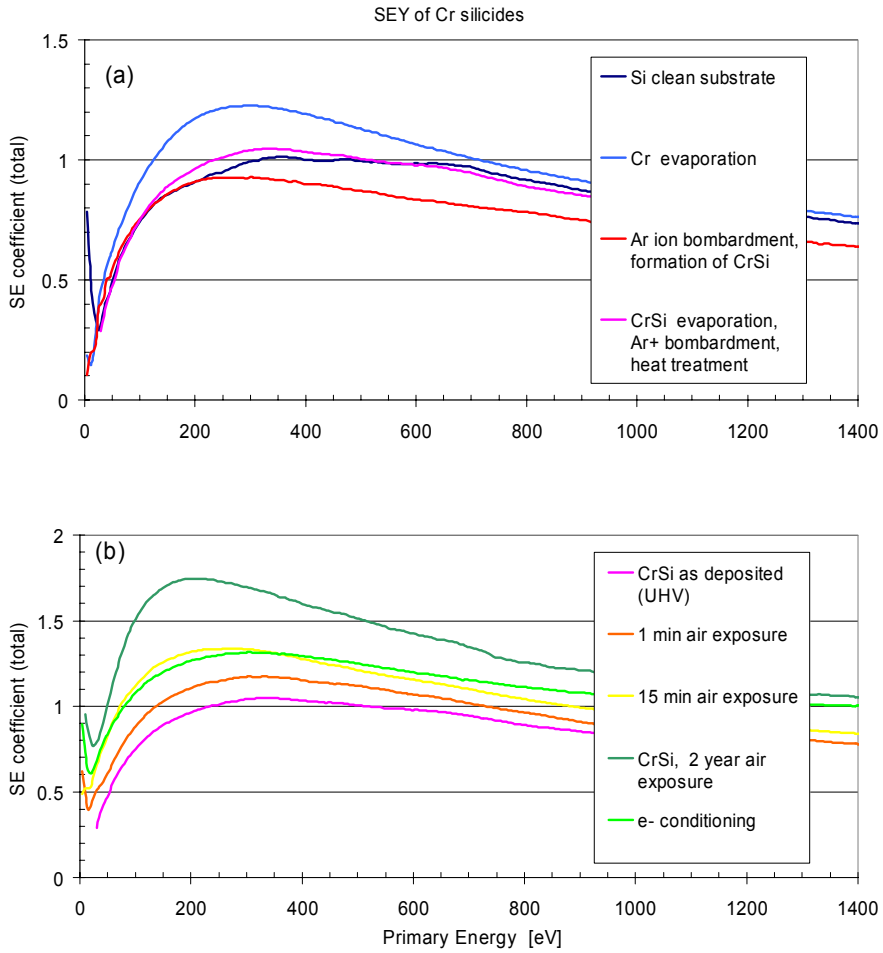

Fig. 2: Secondary Electron Emission Yield of Chromium Silicides

Panel (a), first stages (Cr evaporation and ion mixing by Ar^+ bombardment) and final CrSi coating after several consecutive Cr evaporations, Ar ion bombardments, and heat treatments. In panel (b) two CrSi samples with different air exposures.

2.3.2 Energy Distribution of Secondary Electrons and Model of SEY

As shown by Fig. 2, and 3, for most materials, SEY is a very smooth function of primary energy and can be determined by a few points as indicated in Fig. 3: E_1, the first crossover energy ($\sigma(E_1) = 1$), the maximum (E_m, σ_m), and E_2, the second crossover energy, or $\sigma(E_p = 1500\ eV)$ if E_2 is higher. Thus, there are in the literature several model functions[12–14] more or less simple, more or less empirical, with few adjustable material parameters that can be used in the computer simulation of SEY. However, the model should have enough parameters and flexibility to represent different materials and surface conditions and to allow studying the independent influence of different parts of the curve $\sigma(E_p)$ on the MPT. As mentioned above, a minimum set of four parameters seem to be necessary, plus at least one more for taking into account the dependence on incident angle (in its simpler factorizable expression).

The distribution in energy of the emitted secondary electrons is however what we would like to consider now. Energy distribution curves (EDC) or energy spectra of secondary electrons present always the general shape shown in Fig. 4. To each point of a SEY curve like that in Fig. 3, i.e., to each value of primary energy E_p there corresponds an energy spectrum like those in Fig. 4. In the usual basic interpretation, three main contributions are distinguished.

The peak at the same energy than primary electrons is due to these same electrons backscattered elastically by the surface (mostly in one collision). The width of the peak, i.e., its energy dispersion is due to the finite resolution of the measuring instrument (electron gun + energy analyser). They are emitted in all directions but preferentially in a mirror-like reflection direction. The number of elastics per primary impacting electron, i.e., the corresponding elastic SEY coefficient σ_e varies with primary energy as shown in Fig. 3. At least two parameters are necessary for this E_p function. Material dependence of these parameters might be small or a function of average atomic number. The limit of $\sigma_e(E_p)$ for $E_p \rightarrow 0$ is very difficult to measure and is not clear[15].

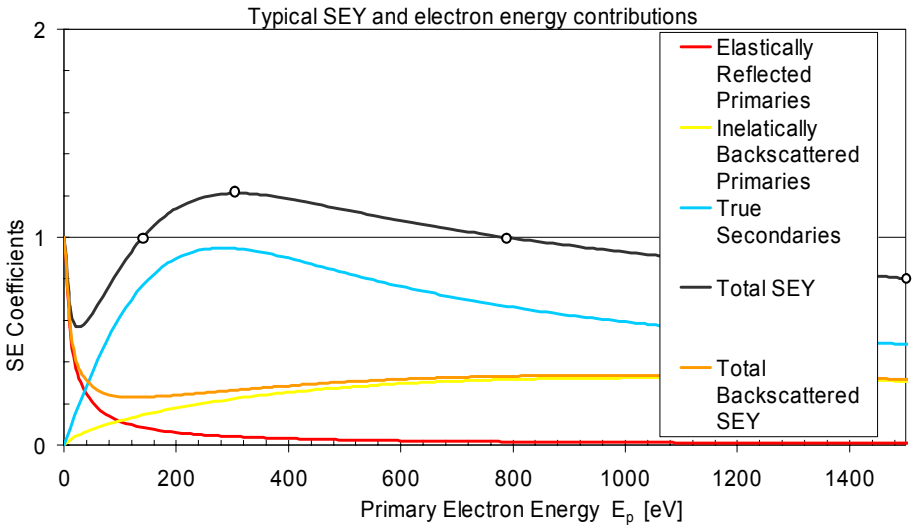

Fig. 3: Typical Primary Energy Dependence of Different SEY Coefficients

They could represent those of clean Cu after electron conditioning and for normal incidence. Zero limit of elastic electrons coefficient might be less than 1, difficult to measure. Definition of backscattered coefficient is usually arbitrary. Here is based on fitting energy distribution curves or spectra of secondaries.

Some impacting primary electrons are backscattered with some energy loss after very few collisions. They appear in the energy spectrum at the corresponding decreased energy forming an extended smooth background behind the elastic peak, as indicated in Fig. 4. This spectrum may have some fine structure due to discrete energy losses (material quantum resonances) completely negligible at the approximation level considered here. Backscattered electrons are also emitted preferentially in a mirror-like reflection direction. The corresponding coefficient σ_b varies with primary energy as shown in Fig. 3. At high energies (500 – 2000 eV) it has a nearly constant value between 0.15 – 0.6 depending of the material (at very high energies decreases with E_p)[(12)]. At least three parameters are needed to describe these variations. Material dependence of these parameters might again be a function of the atomic number alone.

Most of the energy losses undergone by scattered primaries end up creating true secondary electrons. Electrons bound to atoms of the material acquire sufficient energy to get free, diffuse to the surface, and escape to the vacuum. Energetic secondaries may also create more secondaries, thus the true-secondaries spectrum has an increasing intensity towards low energies with a characteristic shape shown in Fig. 4. It has a maximum at ~ 5 eV above vacuum level, produced by the escape probability through the surface energy barrier. True secondary spectrum may also show fine structure: Auger electron emission, conduction band density of states, tunnelling through discrete surface energy states, …, also entirely negligible. True secondaries are emitted in all directions according to the *cosine* or *Lambert law*, i.e., with no memory of the primary incident direction and with probability proportional to the cosine of the emission angle. The dependence on primary energy of the true secondary SEY coefficicient σ_s is also shown in Fig. 3. This is usually described by four parameters, including incident angle dependence.

The measurement of the true secondary coefficient σ_s separately of the backscattered one $\eta = \sigma_e + \sigma_b$ is not well defined since they are not clearly separable. It has become agreed to define true secondaries as those having energies below 50 eV. However, at the sight of Fig. 4, it is clear that this separating energy should be dependent on primary energy.

There are several reasons for taking into account the main features of the energy distribution of emitted secondary electrons when making a simulation of SEY in a computer model of the multipactor effect. Backscattered electrons ($\eta = \sigma_e + \sigma_b$) represent always an important fraction of the total emission, from 25 to 50 %, but they differ from true secondaries in two important aspects: their energies are much higher and their emission directions are not uniform random but bunch in some extent around the reflection direction. This makes their trajectories in the RF field quite different and probably a different contribution to the multipactor discharge.

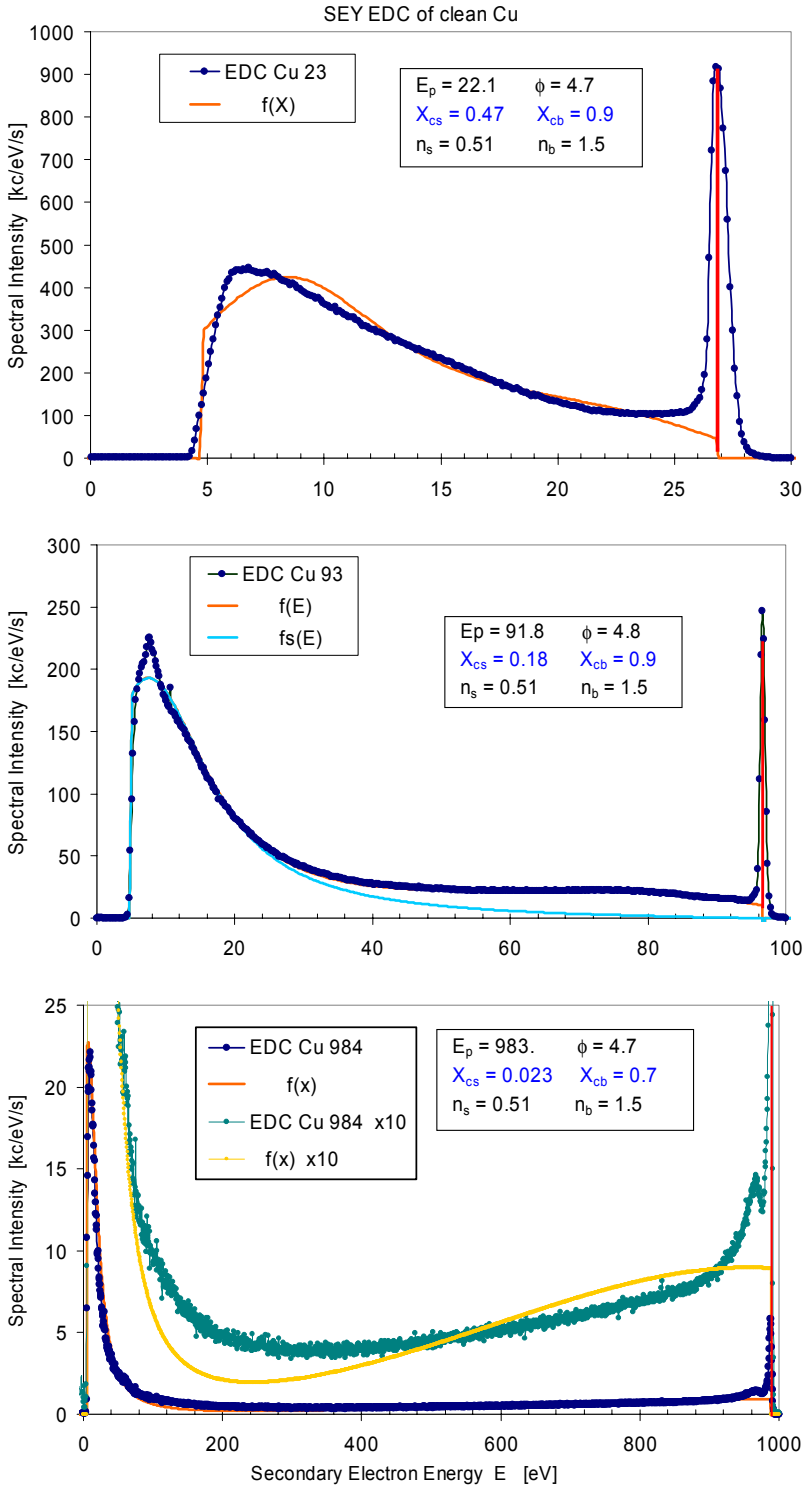

Fig. 4: Energy Distribution Curves of SEY for Cu and Model Contributions

Clean Cu (Ar ion sputtered) not *electron conditioned*. For 30º incidence, 30º emission, and primary energy as in the inset. Secondary energy referred to Fermi level. Work function in the inset. EDC fitted to simple model contributions: true secondaries $f_s(E)$, true backscattered, $f_b = f(E) - f_s(E)$, and elastics, red spike at E_p. $f(E)$ is total secondaries minus elastics. Only two fitting parameters have been used, X_{cs} and X_{cb}, see text.

In a probabilistic (Monte Carlo) simulation of SEY, one basic problem is to choose an emission energy for the emitted electron in a stochastic process with probability distribution like those of Fig. 4. Let $f(E)$ be the normalized secondary spectrum ($\int_0^{E_p} f(E)\cdot dE = 1$) for a given E_p and $F(E) = \int_0^E f(E')\cdot dE'$ the corresponding cumulated probability function. This function has an inverse function $G = F^{-1}$ such that $E = G(u)$ if $u = F(E)$. Therefore, if u is uniformly distributed in (0, 1) then E is distributed in (0, E_p) with the probability distribution

f(E). Since uniform random numbers generators are easily available, the point for a fast problem-free secondary energy generator is in finding a simple analytical expression for *G(u)*. The following phenomenological functions:

$$E/E_p = [(^2/_\pi)\cdot arctan\{\sqrt{[tan((^\pi/_2)\cdot X_{cs})\cdot tan((^\pi/_2)\cdot u)]}\}]^{1/n_s}$$

$$E/E_p = \alpha^{-1/n_b}\cdot[arccos(1-\beta\cdot u)]^{1/n_b} \qquad \beta = 1-cos(\alpha) \quad \alpha = \pi X_{cb}^{n_b}$$

give the energy distribution of true secondary and backscattered electrons, respectively. They have only two fitting parameters each, (n_s, X_{cs}) and (n_b, X_{bs}), they are nevertheless flexible and able to reproduce adequately the spectra of any material, see Fig. 4. These parameters are functions of E_p and of the material. However, n_s, n_b , and even X_{cb} might be fixed and still have an acceptable simulation of the main features of the spectra. X_{cb} is mainly function of the material average atomic number, and X_{cs} of E_p . These functions have not any physical basis but are only designed to solve the problem: a simple flexible computable *G(u)* function such that *f(E)* is an acceptable representation of the spectrum.

2.4 Summary and Conclusion

SEY of various potential coatings for reduced MPT applications have been studied. The first crossover E_1 and the maximum σ_m are the SEY properties influencing more on MPT. A mean value between air exposed and electron conditioned ones correlates better with MPT, and thus is a criterion to evaluate SEY.
Thin films of nitrides, carbides, or silicides of light transition metals like Ti, V, and Cr deposited by reactive evaporation or sputtering with low energy ion assistance seem to have sufficient low SEY, low surface resistance, good mechanical and thermal properties as to be soundly considered for MPT reduction.
The SEY properties of Ti and Cr silicides were measured for the first time. Cr silicides can withstand very long air exposures without impairing their good SEY properties. The same can be said of a V-5%tTi alloy and its nitrides. This could be a property of V alone.
The energy distribution or spectrum of secondary electrons was studied with the aim of modeling adequately this property in a computer simulation of the multipactor effect. Simple functions are proposed for generating easily this property in a probabilistic (Monte Carlo) model of SEY. Including primary-energy dependence of the number of secondaries, about 15 parameters are used in the model. This number might be reduced to about 5 by many of them having either universal values or simple dependence on material properties as average atomic number.

3 Surface Treatment and Coating for the Reduction of PIM; Contribution of TUD

IHF/TUD is in charge of all the aspects of this ESA activity related to PIM. This distortion is of great importance in satellite communications where high and low powers are involved. It has its origin in the non-linear behaviour of the system which results in the excitation of new frequencies apart from the original ones. Despite the fact that the excited frequencies have low power, they can interfere with the incoming signals of the satellite which are also low power signals. Therefore, the intermodulation distortion generated in the transmitted band of the satellite can seriously affect its received band.
The physics lying behind the PIM problem is not well-understood yet. Some known sources of PIM are poor metal contacts, hysteresis of ferromagnetic materials, microcracks at metal surfaces, etc... . In particular, the generation of PIM at waveguide flanges is of great importance. Normally, the reason for PIM generation at waveguide contacts is the poor metal contact in combination with native oxidation of the waveguide metals and the lack of precision in the fabrication process. Consequently, the metal-to-metal contact becomes non-ohmic and therefore non-linear effects can rise in the system. The physical origin of this non-linear behavior is not completely understood, though it seems that it is originated by transport mechanisms in a Metal-Insulator/Semiconductor-Metal structure such as quantum tunneling or also by microcracks at the surfaces, etc…
The objective of this ESA activity regarding PIM is the study of different coating materials which could improve the surface contact between the flanges. Additionally, a PIM software to simulate this contact and therefore, able to predict the Intermodulation behavior of a waveguide junction with some system parameters is the other aim of the project.

3.1 Experimental Stage

The experimental phase will be devoted to the study of potentially suitable PIM coatings. The criteria for this decision are based on the coating material properties as well as their properties regarding the base material (in this case, Aluminium or Silver). In particular, those materials with intermediate Young's modulus (10-50 GPa) draw a great amount of attention. These materials are easily deformable improving the contact at a given pressure. Low Young's modulus materials like Indium have the problem that once they have been used, the

coating loses its initial behaviour and the initial conditions are not recovered. However, not only the coating materials but also the techniques used for applying these coatings are objective of the present investigation.
Some coating materials under study are:

- Indium
- Cadmium
- Bismuth and its alloys
- Magnesium and its alloys.

Properties like adhesion, corrosion, thermal stability are being investigated. The final research will provide a *database of materials* regarding their use as possible PIM inhibitors at waveguide junctions. Combination of more than one coating is also a field under investigation. This could result in a final coating of appropriate characteristics. Different coating techniques are also being considered. These techniques are:

- Electrochemical plating (DC)
- Electrochemical plating (pulse)
- Thermal evaporation
- Magnetron sputtering

The functionality of these techniques will depend on the specific material to be coated. A good coating material could loose their properties for a given coating technique. The geometry of the samples to be coated is also of importance since it could not fit in a particular facility. Magnetron sputtering is very constraint regarding this aspect. Additionally, the ability of each technique providing a well defined coating thickness must be also taken into consideration.
Surface treatment at the flanges is other field of investigation. This is crucial if the surface contact wants to be optimised. In this way, polishing techniques are important if the roughness of the sample surface wants to be minimised. Changes on the geometry of the surface can be also done. In this way, a high pressure flange can be designed (grooved flange). This flange improves the contact by introducing a bridge around the RF path reducing the whole contact area to be connected and then decreasing the pressure needed to achieve a good contact.

3.2 Software development

Apart from the experimental stage, software simulations will be also performed. A software tool that simulates the surface contact will be used for this objective. The software will be able to provide the relative PIM level with the contact pressure under a conservative error. These are the basic parameters that will be taken into account and the output data that will be provided:

Input data:

1. Power and frequency range.
2. Waveguide geometric and electric properties.
3. Physical properties of the coating material (size, Young's modulus,...)
4. Ambient conditions (temperature, ...)

Output data:

1. Excited frequencies and their power levels in dBm.
2. Intermodulation level for a given excited frequency in function of a system parameter (e.g. signals power).

The software will provide the variation of the Intermodulation with the applied pressure, and the pressure needed to achieve full contact between the flanges. This software will be verificated by means of the experimental stage explained in the previous section.

3.3 Results

After this two-year long project, a database with different coating materials will be provided regarding their PIM characteristics. The coating technique used for the specific coating as well as coating thicknesses will be also provided. The eventual polishing techniques used will be also analysed and examined regarding their PIM behavior. Additionally, the software should be able to predict the intermodulation level variation in function of parameters like contact pressure or roughness.

4. Regulated Electron Gun (REG); Contribution of Tesat-Spacecom

For the multipaction testing, especially in the pulsed / multicarrier case, an electron source is required to provide a sufficient amount of seeding electrons. One of the objectives of this contract is the development of a computer controlled regulated source. A regulated electron gun (REG) is foreseen as a source of free electrons. The energy, the current and the density of the electron beam can be regulated. The current of the beam is monitored with a faraday cup and with a sector device. All currents (cathode, Wehnelt, iris, anode) as well as the voltages (cathode, anode, Wehnelt) are also monitored. The spreading of the beam is adjustable. The REG is controlled by a PC, using a graphical user interface. The main characteristics of the REG are:

- Acceleration potential from 1 eV to 1 keV
- Electron current from 0.3 nA to 42 nA
- TTL trigger.

The REG comprises several subunits, which are:

- The electron gun
- The calibration devices (Faraday- cup, sector device)
- The control electronic (measurement devices, power supplies, ...)
- The controlling PC
- The control software

4.1 Description of Electron Gun

The electron gun is one compact cylindrical unit see Fig. 5. It includes the heating filament (cathode), the Wehnelt cylinder, an iris, a ceramic cylinder and an adapter with thread. The gun can be screwed into a piece of waveguide.
The electrons of the REG are generated with a heating filament - a hair pin cathode. The emitted electron cloud around the cathode is accelerated by the potential difference between the cathode and the anode. The electrons are centred by a Wehnelt cylinder. On the way from the source to the target (sample) the electron beam passes an iris. Depending on the mode of operation, the electron beam is stopped by the target, i.e. the wall of the sample, a Faraday-cup or a sector device.

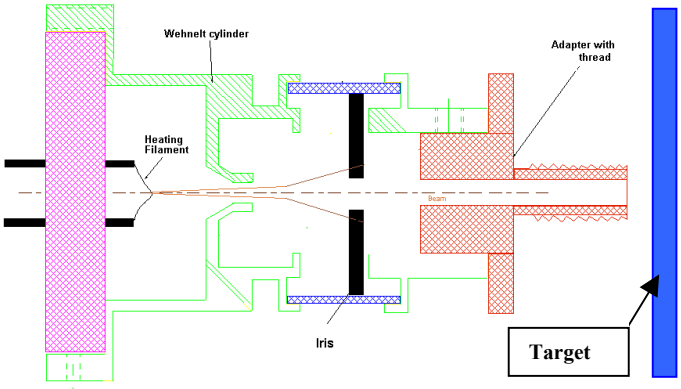

Fig. 5: Cross-sectional View of the Electron Gun

4.2 Calibration Devices

The Faraday-cup measures the beam current at the location of the sample. The sector device is a small plate with a number of insulated small areas – see Fig. 6. The purpose of this sector device is to measure the beam spreading. A focused beam gives only a current in the inner ring(s) of the device - a more spreaded beam gives current in the outer rings, too.

4.3 Control Electronic

All relevant parameters of the REG are controlled: The current and the voltage of the cathode, the Wehnelt, the anode and the iris. Also the currents for calibration (iris, Faraday- cup, sector device) are measured. The

measurement devices are digital voltmeters. The voltmeters, as well as the power supplies are controlled by a bus system such as IEEE-488. The electrical block diagram of the REG is presented in Fig. 7.

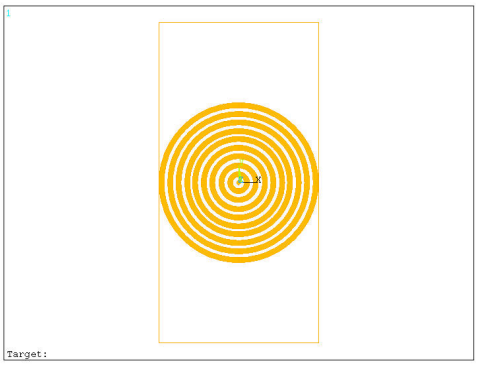

Fig. 6: The Rings of the Sector Device

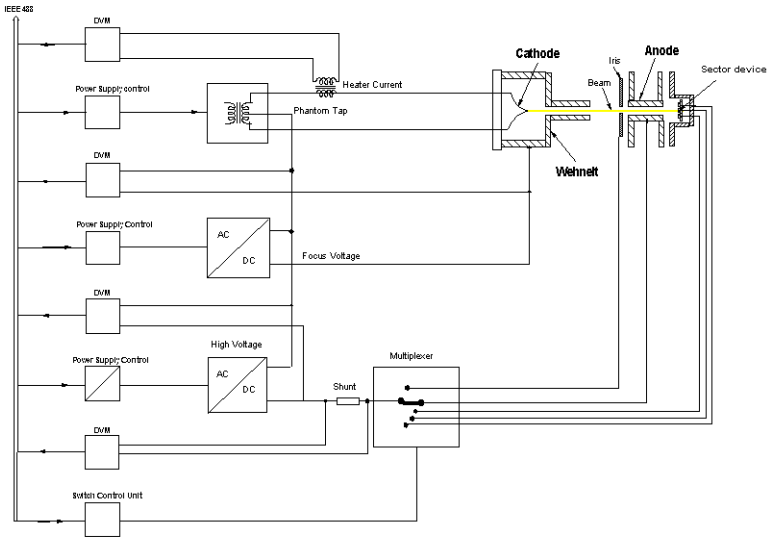

Fig. 7: Blockdiagram of the REG Control Electronics

4.4 PC and Control Software

The standard PC uses an user friendly software running under standard Windows operating system. A schematic of the control software is shown in Fig. 8. The main characteristics of the software are:

- Menu driven handling using mouse or keyboard
- Controls and displays for: cathode heating, accelerating potential, electron spot divergence, emitted electron beam density.
- Display of actual measured values on output screen e.g.: density of electrons emitted, energy spectrum of emitted electrons
- Possibility to save the actual values to standard ASCII files as a ”snapshot”
- In case of errors or warning-situations: corresponding messages on the screen, messages will be stored in a standard ASCII log-file.

The PC performance will be enhanced with a real time extension. Benefits of using a realtime extension are:

- splitting the program in two separate tasks for ”GUI and data handling” and the realtime part for ”control and regulation”,
- deterministic timing of measurements and control independent from “normal” Windows Tasks and actions,
- fast reading of measured values using digital voltmeters

- fast response through programming the power supplies.

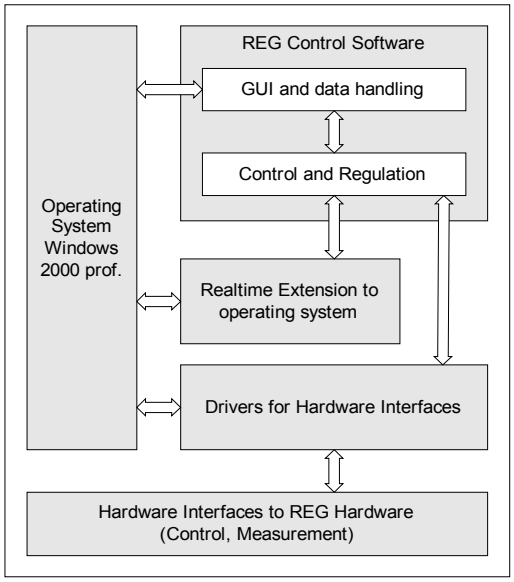

Fig. 8: Scheme of the control software

5. Design and Test of Multipaction Samples; Contribution of Tesat-Spacecom

A set of simple waveguide multipaction samples will be designed, manufactured and tested at Tesat-Spacecom. The inner gap of the samples, which varies between 0.1 and 2 mm, will be adapted to the standard waveguide interfaces (C-Band and X-Band). The gap voltages are calculated accurately by using mode matching technique. The results of the multipaction tests of a first set of alodine treated samples will serve as a reference. A second set of samples with identical gap widths will be provided with selected coatings and measured for comparison and for verification of the software, respectively.
A X-Band test set-up using a ring resonator has already been installed at Tesat-Spacecom facility. The available pulsed peak power at the DUT is currently about 20 kW.
It should be noted, that the PIM test of the samples prepared by TUD will also be performed at Tesat-Spacecom.

6. References

1. "Study of secondary emission properties of materials used for high power RF components in space". L.Galán, C.Morant, F.Rueda, J.M.Sanz, J.Barbero (UAM and CSIC). ESA-ESTEC Contract 6577/85/NL/PB, ESA (1987)
2. "Study of secondary emission properties of materials for high RF power in space". L.Galán, P.Prieto, C.Morant, L.Soriano, and F.Rueda (UAM). ESA-ESTEC Contract 6577/85/NL/PB, ESA (1990)
3. "Coatings to prevent multipactor effect in RF high power components for space". N.Díaz, S.Castañeda, I.Montero, L.Galán, and F.Rueda (UAM and CSIC). ESA-ESTEC Contract P.O.162594(1996), ESA (1998)
4. F.Rueda et al, in "Workshop on Multipactor, RF and DC Corona and Passive Intermodulation in Space RF Hardware, Sep 2000", ESA Publications Division. c/o ESTEC PO Box 299 AG Noordwijk, Holanda
5. A.Woode and J.Petit: ESTEC Working Paper No. 1556 (1989) ESTEC ESA
6. F.Höhn et al: Phys. Plasmas **4**(4) (1997) 940
7. "Development of a computer model for the multpactor effect". L.Galán, M.A.Jiménez, and F.Rueda (UAM). ESA-ESTEC Contract 6577/85/NL/PB 1990/Rider, ESA (1991)
8. LH10, Leybold-Hereaus, Köln, Germany (1985).
9. E.L.Garwin et al, J.Appl.Phys., **61** (1987) 1145
   A.R.Nyaiesh et al, J.Vac.Sci.Technol. A, **4** (1986) 2356
   I.E.Campisi et al, IEEE Trans.Nucl.Sci., **NS-30** (1983) 3363
   E.L.Garwin et al, J.Appl.Phys., **59** (1986) 3245
10. P.Prieto: Doctoral Thesis, Dep. de Física Aplicada. Universidad Autónoma de Madrid. Dic 1992.
11. J.H.Weaver et al, Phys. Rev. B, **29** 3293 (1984).
12. L.Reimer, "Scanning electron microscopy", Springer Series in Optical Sciences **45**, Springer-V (1985) 128
13. A.Schwarz, J. Appl. Phys. **46**, 8 (1990) 2382
14. M.A.Furman, CERN LHC Project Report 180 (1998)
15. N.Hilleret et al, CERN LHC Project Report 472 (2002)
16. C. Vicente, A. Cervelló, M. Mattes, D. Wolk, B. Mottet, D. Raboso, H.L. Hartnagel, J. Mosig, "AO-4026 ITT ESA – Multipactor and Corona Discharge: Simulation and Design in Microwave Components", 4th International Workshop on Multipactor, Corona and Passive Intermodulation in Space Hardware, ESA/ETEC 2003.